Composite Structures

Experimental and numerical study on the mechanical response of Nomex honeycomb core under transverse loading

Longquan Liu [a,b,*], Hai Wang [a], Zhongwei Guan [b]

[a] School of Aeronautics and Astronautics, Shanghai Jiao Tong University, 800 Dongchuan RD., Minhang District, Shanghai 200240, China
[b] School of Engineering, University of Liverpool, Brownlow Street, Liverpool L69 3GQ, UK

ARTICLE INFO

Article history:
Available online 20 November 2014

Keywords:
Flatwise compression
Nomex honeycomb core
Resin effect
Mechanical response
Finite element

ABSTRACT

This paper presents an experimental and numerical investigation on the mechanical response of the Nomex honeycomb core subjected to transverse loading. Here, a series of tensile, stabilized compressive and step-by-step compressive tests were carried out, also a meso-scale finite element modelling method was developed to simulate the resin-paper-resin layered honeycomb cell walls by employing explicit shell elements. Through the analysis of the test results, the brittle fracture behaviour of the phenolic resin coating is recognised as a main reason of the honeycomb collapse. Both the strength and modulus of the honeycomb core in tension are higher than those in compression, due to the local buckling of the thin cell walls at a quite low level of compressive loading. From the numerical analysis, it was found that the volume of the resin coating has a positive effect on the collapse strength of the honeycomb core, however has no influence on the collapse strain. Moreover, the modulus of the resin coating has a positive effect on the collapse strength but a negative effect on the collapse strain. In addition, the strength of the resin coating has positive effects on both the collapse strength and strain of the honeycomb core.

1. Introduction

A honeycomb sandwich is a structure that consists of two relatively thin face sheets bonded to a relatively thick lightweight honeycomb core. The face sheets primarily carry tensile and compressive loads, whereas the core supports the face sheets against buckling and resists out-of-plane shear loads [1–3].

Honeycombs are manufactured from a variety of materials, including Kraft paper, thermoplastics, aluminium, steel, titanium, aramid paper, glass fibre, carbon fibre, ceramics, etc. Each honeycomb material provides certain properties and has specific benefits. The most commonly used core material in aerospace applications is phenolic resin-impregnated aramid paper, known as Nomex® (E.I. du Pont de Nemours Corp., Wilmington, DE, USA) [4–6]. This is mainly due to its flame resistance, good insulating properties, low dielectric properties, large selection of cell sizes, low strength/weight ratio, formability and parts-making experience. Examples of the applications of Nomex honeycomb core sandwich in airplane are floors, doors, wing flaps, wing-body fairings, rudders, overhead stowage bins, ceiling or sidewall panels, engine cowls, spoilers, nacelles and radomes, etc. [3,6–8].

Honeycomb sandwich structures have high specific out-of-plane compression and shear properties, as well as outstanding energy absorption characteristics. A drawback, however, of using honeycombs as a sandwich core structure is the tendency of the honeycomb to crush during transverse impact loading caused by runway debris, hailstones, dropped tools, etc., due to the rather low mechanical properties of honeycomb structures in the out-of-plane direction [9–14]. The support of the honeycomb core to the facing will decrease significantly after the core is collapsed. Therefore, the collapse resistance of the honeycomb core under flatwise compression is a key factor to be considered.

Extensive researches were conducted on the mechanical behaviour of the honeycomb core with homogeneous cell materials subjected to flatwise compressive loading. Gibson and Ashby [15] provided a comprehensive review on the mechanical behaviour of cellular solids and analytical studies of the stiffness and strength of the honeycomb core under transverse loading. Many studies [16–20] were undertaken on the buckling and post buckling process of transversely-loaded aluminium honeycombs by using both experimental and numerical approaches.

However, most of these research methods and outputs are only applicable to the honeycomb cores made of homogeneous

* Corresponding author at: School of Aeronautics and Astronautics, Shanghai Jiao Tong University, 800 Dongchuan RD., Minhang District, Shanghai 200240, China. Tel.: +86 21 34205479.
E-mail address: liulongquan76@sjtu.edu.cn (L. Liu).

materials, which may not be the case to the Nomex honeycomb cores. The basic material of the honeycomb core is phenolic resin-impregnated Nomex aramid paper and the cell wall is essentially a laminated structure due to its manufacturing processes [21,22]. The paper substrate has very good ductile properties (the elongation at break from 0.07% to 0.12%), however the phenolic resin coating is rather stiff and brittle (the ultimate elongation of only 0.02 with hardly any plastic strain). Therefore, the mechanical response and failure mode of the Nomex honeycomb core under transverse loading are quite different from those made of metals.

Normally, the aramid paper, resins and the honeycomb products are manufactured by different manufacturers. Honeycomb suppliers just provide global properties of whole honeycomb structures [7], such as the collapse strength and the out-of-plane shear modulus, and keep the recipe of the honeycomb commercially confidential. Thus, the raw material data of the constituents of the cell wall, phenolic resin and aramid paper are not easily accessible in public domain [23]. Also, the properties of the Nomex honeycomb cell wall are dependent on both the constituent materials and their proportion.

As the result, it is necessary to undertake experimental tests to investigate the mechanical properties of the honeycomb core under transverse loading. However, the pure experimental approach is rather costly and time consuming. Therefore, a lot of research work has been carried out to develop reliable simulation procedures in order to predict the damage tolerance behaviour of the honeycomb sandwich structures efficiently.

In the finite element modelling, the multi-cellular core is usually modelled as equivalent spring elements [24–27] or equivalent three-dimensional continuum elements [13,28–35] in order to reflect the energy-absorbing and impact resistance of honeycomb sandwich structures. Instead of considering the real cellular structure, the sandwich core is analyzed in terms of its effective properties. Although the effective material data of honeycomb core blocks under transverse loading can be usually obtained through flatwise tests [36,37], there exist two problems to be overcome with this method. Firstly, tests need to be conducted for each type of cores with different parameters, such as height, cell size, wall thickness, resin ratio (relating to the core density), etc. Secondly, this approach can only be used to simulate the global responses of the honeycomb sandwich structures phenomenologically, which does not reflect the real failure mechanisms. One reason is that the influence of the local core failure mechanism is not considered in the equivalent continuum model, and the other one is that it may be difficult to simulate the exact damage progression due to the discontinuous surfaces of the honeycomb core in contact with the face sheets. Thus, it is very difficult to account for local failure modes of the hexagonal cell structures [38–41]. Nevertheless, these local effects are important from case to case, where the damage tolerance is of interesting.

The afore-mentioned limitations can be overcome by finite element modelling of the honeycomb core explicitly using shell elements to obtain more realistic distributions of stresses and strains. Some scholars [3,6,7,14,42–45] proposed meso-scale modelling methods, which treat the cell walls of the honeycomb core explicitly through two-dimensional shell elements. Using the test results of the cell wall of resin-impregnate Nomex paper as the input of material properties, these meso-scale models can be used to simulate the failure process of the Nomex honeycomb core more realistically and to investigate the influence of the geometry parameters on the mechanical properties of the honeycomb core. In addition, they can be used in more general load cases, such as impact and bending. However, due to the lack of material data of the constituents of the honeycomb cell walls and the unknown layered features of the Nomex cell walls to be considered in meso-scale models, extensive tests are still required to investigate the cores with different material properties and volumetric ratios of the aramid paper and phenolic resin. Roy et al. [45] and Foo et al. [23] studied the material properties of the aramid paper and phenolic resin used in the honeycomb core and however, in their meso-scale models only equivalent material properties were used for the shell elements which could not help investigate the failure mechanisms properly.

Therefore, it is necessary to develop a finite element model to correctly represent the layered structure of the core, which can be further used to investigate the failure mechanisms and the effects of mechanical properties of the base materials on structural behaviour of the Nomex honeycomb core. In this paper, a series of tests are firstly presented to investigate the mechanical response of the honeycomb core under transverse loading. The experimental results are analyzed and discussed thoroughly to help understand the failure mechanisms. Then, numerical models with considerations of the geometrical and material conditions of the honeycomb core is proposed and developed to predict the influence of the volume and properties of the paper substrates and the resin coatings on the mechanical properties of the core. The finite element simulations show reasonably good correlation with the related experimental results. In addition, various theoretical approaches are evaluated and compared with each other.

2. Experimental study

2.1. Specimen description

Two different types of Nomex honeycomb-cored sandwich specimens were investigated in the present work. They both have in-plane dimensions of 50 mm in length, 50 mm in width, and the heights of the cores are 20 mm and 14 mm, respectively. All the geometry and material parameters of the sandwich specimens are the same, except for the height of the honeycomb core. Here, the geometry of the sandwich with a height of 20 mm is illustrated in Fig. 1. The facesheets of the honeycomb sandwich structure are $[45/-45]_5$ carbon fibre fabric/epoxy laminates with a nominal ply thickness of 0.188 mm.

The core consists of regular hexagonal Nomex honeycombs with cell size and density of the honeycomb core being 3.2 mm and 48 kg/m^3, respectively. The basic material of the honeycomb core is phenolic resin-impregnated Nomex aramid paper. The honeycombs were manufactured in an expansion process from Nomex Type 412 aramid paper with nominal thickness of 0.05 mm and an areal density of 40 g/m^2. The three material directions of the honeycomb core are illustrated in Fig. 1(b), referred as the L-direction (ribbon direction), W-direction (direction perpendicular to the ribbon), and the out-of-plane direction as the T-direction (through-the-thickness direction). The cell walls oriented in the L-direction are twice as thick (double cell walls) as the other cell walls (single cell walls), which is a result of gluing the paper sheets in the manufacturing process [21,44–47].

The nominal stabilized compressive strength of the honeycomb core is 1.72 MPa, whilst the tensile strength of the Nomex 412 aramid paper in machine and cross-machine directions are 88 MPa and 35 MPa, respectively. The shear modulus in L and W directions are 35.2 and 19.4 MPa respectively, while the elastic moduli in the machine and cross-machine directions are 3.1 and 1.6 GPa, respectively. Moreover, the elongation at break in the machine and cross-machine directions are 9.6% and 6.5%, and the Poisson's ratio is about 0.3.

2.2. Flatwise compressive tests

Flatwise compressive strength and modulus are fundamental mechanical properties of sandwich cores that are used in designing

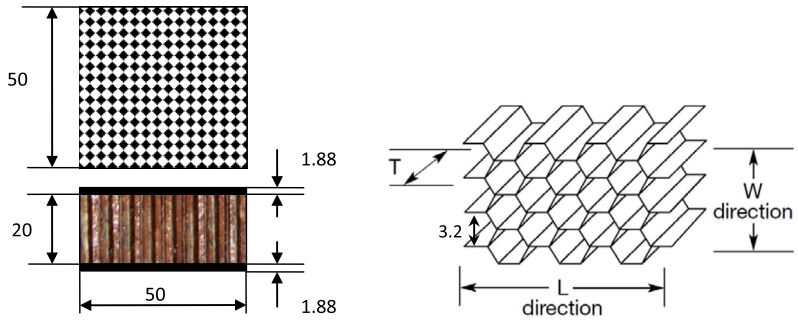

Fig. 1. Geometry of the honeycomb sandwich specimen (dimensions in mm). (a) dimensions of the sandwich, (b) dimensions of the honeycomb core.

sandwich panels. Since the stabilized honeycomb core with facesheets represents the nature of sandwich, such specimens were tested in order to prevent possible local crushing.

In order to determine the mechanical response of the stabilized honeycomb core subjected to flatwise compressive loading, the sandwich specimens were compressed on a universal material testing machine (MTS-SANS 5105) according to the ASTM C 365 [48], as shown in Fig. 2. Five repeated tests were conducted for each type of specimens (one test of the 14 mm high sample was failed abnormally). A plate was fixed to the upper moveable head, which can only move along the up-and-down direction. A spherical seat was installed on the lower stationary head in order to self-align the testing machine and eliminate possible eccentric load. The test samples were compressed quasi-statically under displacement control at a constant cross-head speed of 0.2 mm/min to eliminate the dynamic effect.

The load and displacement were measured with a built-in load cell and transducer of the testing machine. The data were recorded through a computer connected to the testing machine at a sampling rate of 10 data per second.

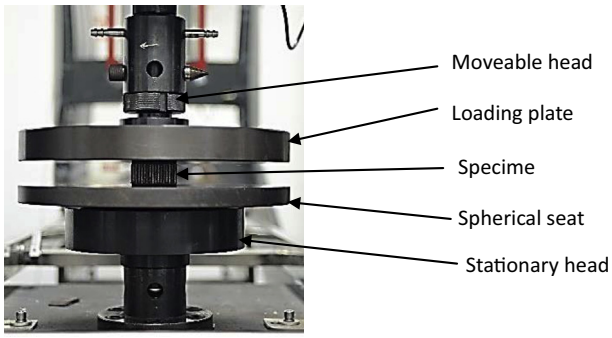

Fig. 2. Test setup of a honeycomb core under flatwise compression.

2.3. Compressive tests with loading cycles

A series of step-by-step compressive tests were also performed on the sandwich specimens with 20 mm honeycomb cores. The specimens were unloaded completely through four loading cycles, which are related to the elastic deformation, softening, crushing and densification, respectively.

2.4. Tensile tests

To obtain the tensile properties of the honeycomb core, five cores with 20 mm height were quasi-statically tested in accordance with the ASTM C 297/C 297M-04 [49], which is shown in Fig. 3. A uniaxial tensile force normal to the plane of the sandwich was transmitted to the sandwich through the two steel loading blocks with 60 mm $\times$ 60 mm interface area. The facesheets of the sandwich specimen were bonded to the centre of loading blocks to minimize load eccentricity. The loading fixtures were cross-arranged to self-align the specimen and eliminate the secondary bending to avoid premature failure. An extensometer was attached to the surface of the steel blocks to measure the deformation of the honeycomb core during loading. The deformation of the steel block and the facesheets were ignored. The test was also under displacement control at a constant cross-head movement of 0.2 mm/min, again to minimize possible dynamic effect.

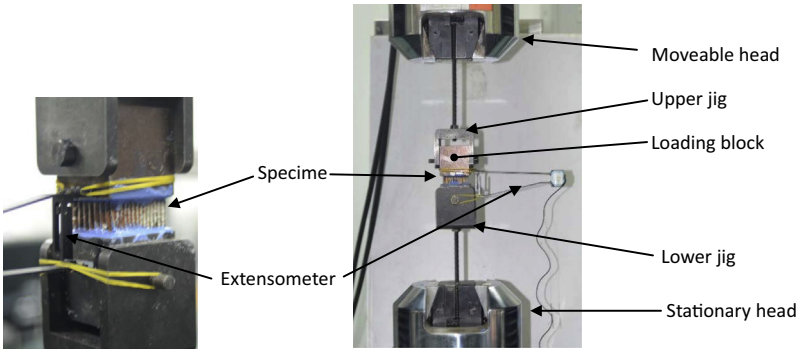

Fig. 3. Setup of the tensile test for honeycomb core. (a) t = 20 mm, (b) t = 14 mm.

3. Analysis and discussion of experimental results

3.1. Compressive test results

3.1.1. Load–displacement curves of the honeycomb core in compression

The load–displacement curves are shown in Fig. 4. From the figure, it can be seen that the collapse loads of the honeycomb cores with different core heights are almost the same, both are about 4300 N, which means the related collapse strength are about 1.72 MPa. The collapse displacement of the honeycomb core with 20 mm height is 0.43 mm and that of the honeycomb core with 14 mm height is 0.3 mm, which indicate both honeycomb cores collapse at the same strain of 0.02. The densification displacements corresponding to these two honeycomb cores are 14 mm and 9 mm, respectively.

Since the load–displacement relationships of all the specimens with the same core height are similar, only one typical load–displacement curve of the honeycomb core with 20 mm height is discussed in detail, as shown in Fig. 5(a). From the curve, the flatwise compressive loading can be generally divided into four stages. The compressive load increases almost linearly up to the peak point of 4300 N with corresponding displacement of 0.43 mm. Then the load drops significantly to an initial plateau load of 2080 N with the related displacement of 0.97 mm, as shown in Fig. 5(b). Following that, it is a hardening stage with the load being increased to the densification point of 3470 N with the displacement of 13.8 mm. The test was terminated at a load level of 4950 N (with a displacement of 16 mm), which is well into the densification stage. From Fig. 5(b), the initial stiffness of the honeycomb core under stabilized flatwise compressive loading is about 11,870 N/mm and therefore, the stabilized flatwise compressive modulus is about 95 MPa.

3.1.2. Crushing strength of honeycomb core

From Fig. 4, it can be seen that the crushing loads of the honeycomb core are between 2000 N and 3000 N, which give the corresponding crushing stresses between 0.8 MPa and 1.2 MPa. However, it is difficult to identify a precise crushing stress of the honeycomb core since there is only a very short plateau stage, followed by continuous hardening until the densification. The hardening was partially attributed to the air pressure inside the honeycomb, since the honeycomb core and the facesheets were glued together and the air was sealed inside.

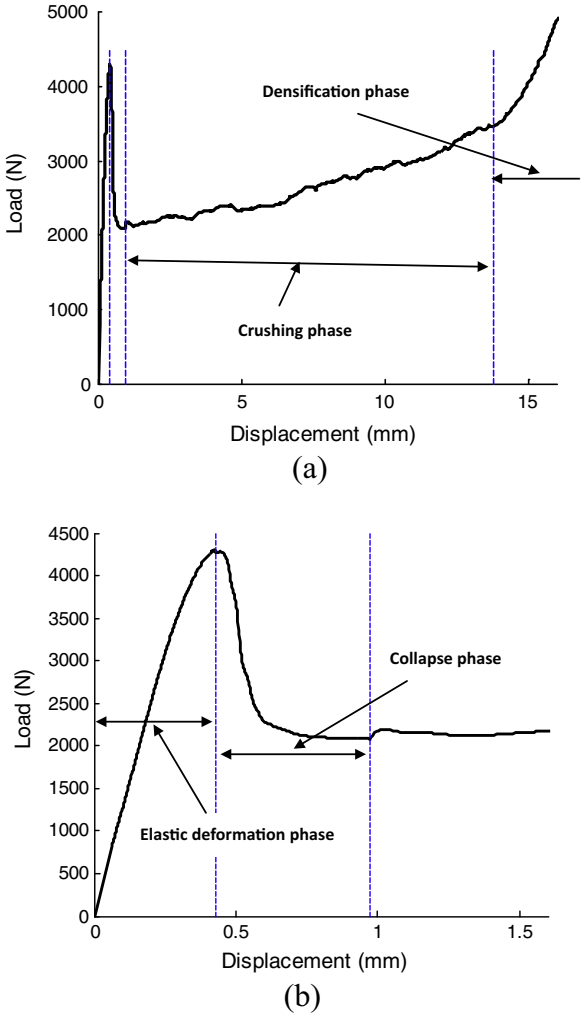

Fig. 5. Load–displacement curves of the specimens under a flatwise compressive load. (a) 0 mm, (b) 0.3 mm, (c) 0.43 mm, (d) 1 mm, (e) 6 mm, (f) 10 mm.

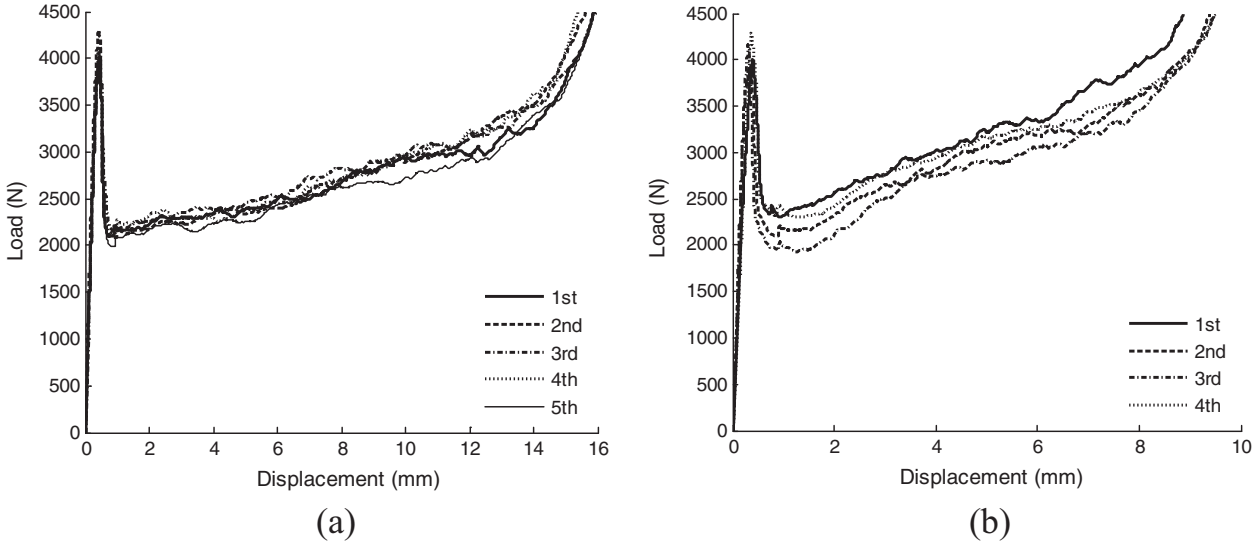

Fig. 4. Load–displacement curves of the specimens under flatwise compressive load. (a) Load–displacement curve through the whole loading stage, (b) load–displacement curve at the initial loading stage.

3.1.3. Deformation and failure process of honeycomb core in compression

Fig. 6 shows a typical deformation sequence of honeycomb cell walls during flatwise compressive loading. While Fig. 6(a) shows the initial configuration, Fig. 6(b) shows that there is no obvious buckling on the cell walls as the compressive displacement is 0.3 mm. Fig. 6(c) shows the cell wall starts to crack and fold as the compressive displacement is raised to 0.43 mm, with the local failure randomly distributed on the middle-high region of cell walls. From Fig. 6(d)–(f), the failure of the cell walls becomes increasingly clear with the compressive displacement. The failure just occurred in one location of each cell wall. The cracking sound was heard continually when the load dropped abruptly after the first peak.

3.2. Flatwise compressive test results with loading cycles

During the first loading cycle, both the loading and unloading curves are fairly close with each other with a small hysteresis. There is no damage in the honeycomb core. In the second loading cycle, the loading curve matches with the first unloading curve very well, whilst the unloading process does not take the load back to zero immediately, i.e. the deformation is of visco-elastic nature. The honeycomb core takes a short time to recover to its original height.

During the third loading cycle, the loading trace is clearly different with the second unloading path, which indicates that there are some damages introduced in the second loading cycle. The peak load of the loading in this cycle is similar to that of the unloading value in the second cycle. Although there is no apparent collapse, the unloading process takes a long time to back to zero, i.e. there is a significant visco-elastic deformation associated with energy dissipation (Fig. 7(a)). The spring back characteristics of the honeycomb core under transverse loading are beneficial to prevent the delamination between the facesheets and the core to some extent. In the fourth loading cycle, the loading is again initiated from the origin, as shown in Fig. 7(b). However, the unloading starts at a point well into the densification stage. As the result, there is a large permanent deformation (>13 mm) in the honeycomb core.

Therefore, the resin coating fracture appears to be the main reason of the collapse of the Nomex honeycomb core. Measures should be taken to postpone the failure of the resin coating in order to enhance the collapse strength and strain of the honeycomb core under flatwise compressive loading.

3.3. Tensile test results

3.3.1. Load–displacement curves and failure modes

The load–displacement curves of the five tensile tests are shown in Fig. 8, with a typical failure mode of the honeycomb cores under tensile loading shown in Fig. 9. From Fig. 8, it can be seen that the load varies linearly with the displacement in general. The specimens fail instantly with cracking noise and dropping the load to zero.

The maximum loads, the related displacements and the loads at the displacements of 0.1 mm ($F_{0.1}$) and 0.05 mm ($F_{0.05}$) of the five specimens are shown in Table 1.

Therefore, the average equivalent tensile strength of the honeycomb core is about 2.13 MPa. The average initial stiffness of the specimens is 16,240 N/mm, and the equivalent tensile modulus of the honeycomb core is 130 MPa. The equivalent tensile strength of the core is about 1.24 times of the equivalent compressive collapse strength and the equivalent tensile modulus is about 1.37 times of the equivalent compressive one.

3.3.2. Thickness of the resin layer

The weight and density of the Nomex T412 aramid paper are 40 g/m^2 and 0.74 g/cc, respectively, the average thickness of the paper is 0.054 mm. The cell size of the honeycomb core is 3.2 mm. Therefore, the relative density of the core without resin can be calculated as 0.045 using Eq. (1) below for a double thickness honeycomb [15]:

$$\frac{\rho^*}{\rho} = \frac{8}{3}\frac{t}{c} \tag{1}$$

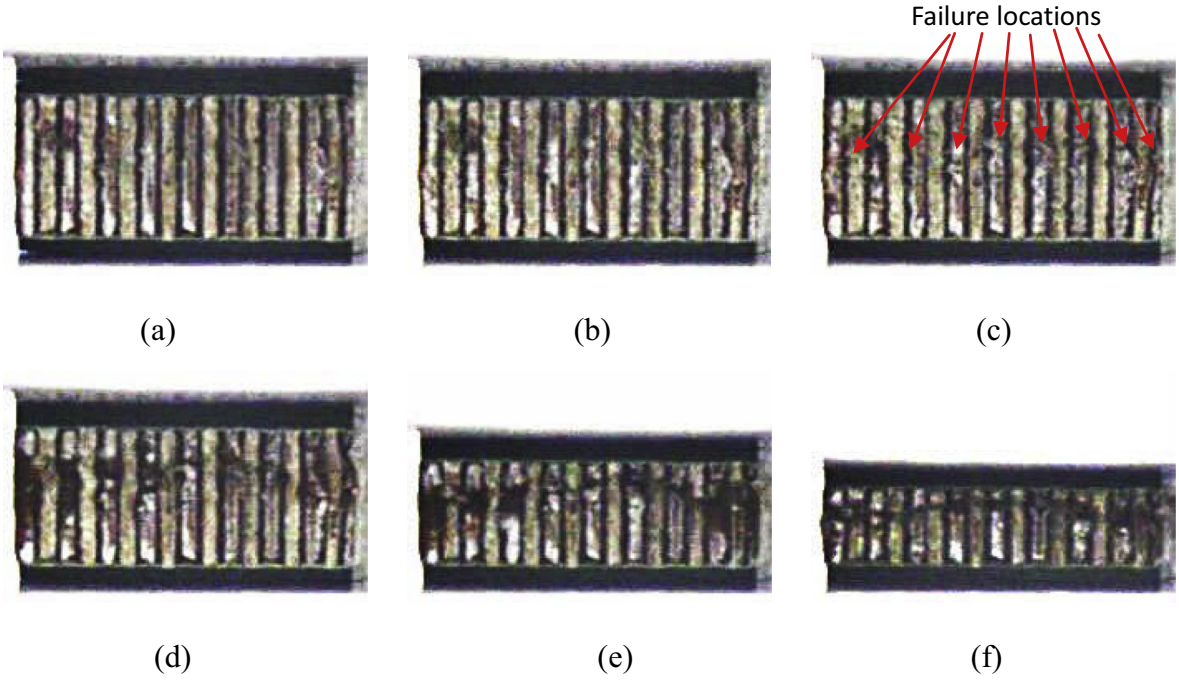

Fig. 6. Deformation process of the honeycomb core sandwich structure under a flatwise compressive load. (a) Load–displacement curves with the displacement no more than 2 mm, (b) load–displacement curves of the whole loading scale.

where t is the thickness of the single cell walls and c is the cell size of the honeycomb core.

Thus, the total weight of the Nomex T412 aramid paper in 1 m^3 honeycomb block is 33.3 kg. Therefore, the weight of the phenolic resin in 1 m^3 honeycomb block is 14.7 kg.

The density of the phenolic resin is about 1380 kg/m^3 [45,46]. As the result, the volume of phenolic resin in 1 m^3 honeycomb block is about 0.01 m^3, which indicates that the contribution of the phenolic resin to the relative density in the honeycomb block is about 0.01. In addition, the relative density of the honeycomb core is 0.055.

Assume the resin is uniformly distributed on the surfaces of both the honeycomb single and double cell walls, the relative density of the honeycomb core with a uniform wall thickness can be calculated as 0.016 mm according to Eq. (2) below [15]:

$$\frac{\rho^*}{\rho} = \frac{2}{\sqrt{3}}\frac{t}{l} \tag{2}$$

where l is the edge length of the cells.

Therefore, the thickness of the resin layer on each side of the cell walls is 0.008 mm, the total thickness of the resin-dipped honeycomb single cell wall is 0.07 mm, and the total thickness of the resin-dipped honeycomb double cell wall is 0.124 mm.

Since the equivalent tensile and compressive modulus of honeycomb core are 130 MPa and 95 MPa, respectively, the equivalent tensile and compressive modulus of the resin-impregnated Nomex™ paper along the thickness direction are thus about 2362 MPa and 1727 MPa, respectively.

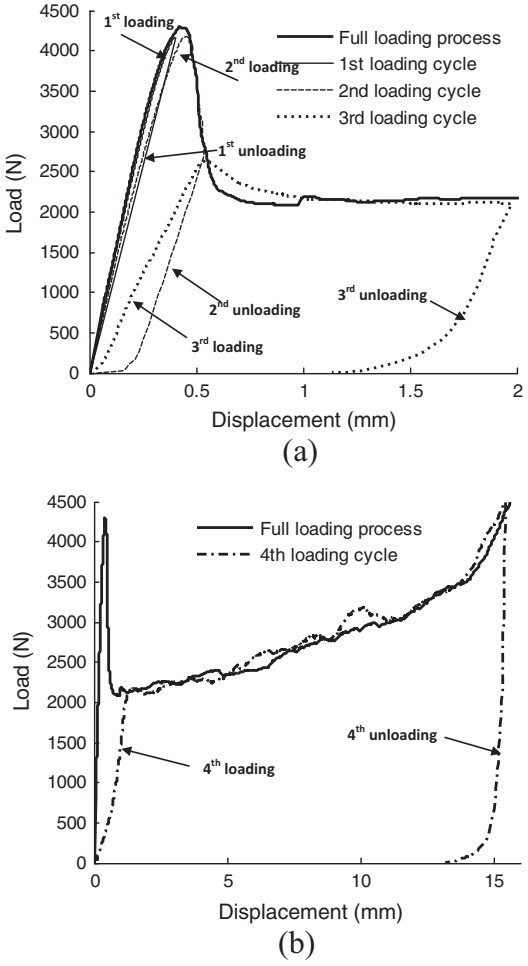

Fig. 7. Load–displacement trace of the honeycomb core sandwich subjected to four loading cycles of flatwise compression.

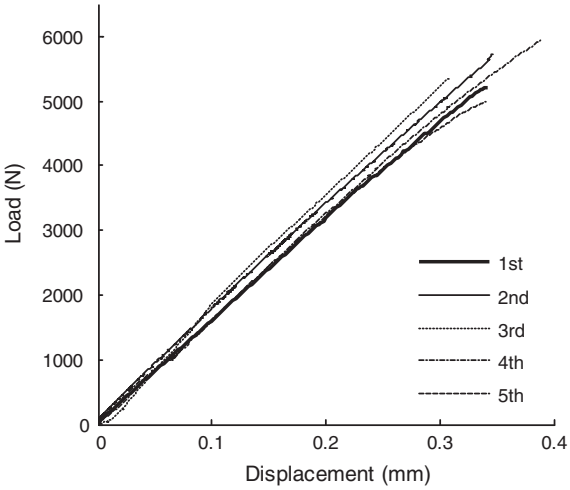

Fig. 8. Load–displacement curves of the tensile tests.

Fig. 9. Failure mode of the tensile test.

3.3.3. Tensile modulus o the resin

According to its manufacturing process, the thickness of the honeycomb core should be coincident with the cross-machine direction of the aramid paper [21,45]. The tensile modulus of the aramid paper with a mean thickness of 0.054 mm is 1.6 GPa in the cross-machine direction. The equivalent tensile stiffness of the honeycomb core with 50 mm in length, 50 mm in width and 20 mm in height is 16,240 N/mm, according to the tensile test results. Thus, the elastic modulus of the resin is about 5.8 GPa.

3.4. The reason of the increase of the crushing stress during compression

Assuming the resin and the aramid paper to be incompressible, the total volume of the resin and paper in the honeycomb core is 2750 mm^3. The total volume (v_1) of the air inside the honeycomb core before compression can be obtained as 47,250 mm^3. Furthermore, the volume of the air inside the honeycomb core after the compressive displacement of 13 mm (v_2) is found to be 14,750 mm^3.

Ignoring the influence of the temperature during quasi-static compression, the load caused by the rise of air pressure inside the honeycomb core can be calculated according to the ideal gas equation of state, Boyle's law, as Eq. (3):

$$P_1 v_1 = P_2 v_2 \tag{3}$$

Therefore, the pressure inside the honeycomb core related to the compressive displacement can be calculated as 0.32 MPa.

The load introduced by the rise of air pressure due to the compressive displacement of 13 mm can be obtained as 558 N.

Table 1
Load and displacement results of the tensile tests.

	Specimen-1	Specimen-2	Specimen-3	Specimen-4	Specimen-5	Mean value
Max load (N)	5069	5576	5204	5854	4859	5313
Max displacement (mm)	0.342	0.346	0.308	0.389	0.34	0.345
$F_{0.1}$ (N)	796	908	797	823	799	824
$F_{0.05}$ (N)	1554	1782	1728	1550	1568	1636

In the same way, the load introduced by the air pressure related to the compressive displacement of 1 mm can be calculated as 14 N. Therefore, the force difference introduced by the air pressures in relation to the compressive displacements of 13 mm and 1 mm is 544 N. However, this force difference, according to the test results shown in Fig. 7, is about 1014 N, which is much greater than the air pressure load. This indicates that, together with the air pressure, some other structural aspects also play similarly important role on the increase of crushing resistant force during compression, which needs to be further studied.

3.5. Theoretical predictions

3.5.1. Elastic buckling stress

The elastic buckling stress of the regular hexagonal honeycomb with double cell walls according to Zhang and Ashby [51] can be calculated as:

$$\frac{(\sigma^*_{el})_3}{E_s} = \frac{5.73}{(1-v_s^2)}\left(\frac{t}{l}\right)^3 \frac{5}{cos30^\circ(1+sin30^\circ)} \approx 22\left(\frac{t}{l}\right)^3 \tag{4}$$

in which the E_s is the elastic modulus of the material of the honeycomb core and v_s is the Poisson's ratio.

The initial buckling stress of the honeycomb core according to Wang [52] can be calculated using Eq. (5) below:

$$\sigma^*_e = 5.34E_s\left(\frac{\rho^*}{\rho_s}\right)^3 \tag{5}$$

Substituting the elastic modulus of the cell wall material (2632 MPa), the single cell wall thickness (0.07 mm), the edge length of the hexagon (1.85 mm) and the relative density (0.055) into Eqs. (4) and (5), the elastic buckling stress can be obtained as 3.14 MPa and 2.34 MPa, respectively. According to these two equations, the honeycomb walls start buckling as the compressive strain are about 0.0012 and 0.009, respectively, which give the relative displacements of 0.024 mm and 0.018 mm. This indicates that the cell walls start to buckle in the very beginning of the loading process. However, it is not easy to monitor the buckling phenomena in this early stage of the test.

3.5.2. Collapse stress and strain

The brittle bucking stress of the honeycomb core according to Gibson and Ashby [15] can be calculated as follows:

$$\frac{(\sigma^*_{cr})_3}{\sigma_{fs}} \approx 12\left(\frac{t}{l}\right) \tag{6}$$

in which σ_{fs} is the material strength.

Substituting the tensile strength of the phenolic resin coated aramid paper (2.13 MPa), the thickness of the double cell wall (0.124 mm), and the edge length of honeycomb (1.85 mm) into Eq. (6), the collapse stress can be obtained to be 1.71 MPa, which is close to the collapse strength of honeycomb core, 1.72 MPa, in this study.

According to the analytical equation provided by Volynskii et al. [53], the critical buckling strain of thin coatings deposited on soft polymer substrates can be obtained using the following equation:

$$\varepsilon = \sqrt[3]{\frac{9E^2}{64E_1^2}} \tag{7}$$

in which the E, E_1 are the Young's modulus of the aramid paper substrate and the resin coating, respectively.

Substituting the Young's modulus of the resin, 5.8 GPa, and that of the aramid paper, 1.6 GPa into Eq. (7), the collapse strain can be obtained to be 0.221, which is much larger than the collapse strain of 0.0215 in this study. This indicates that the analytical solution for instability analysis of thin coatings deposited on soft polymer substrates is not adequate for the buckling problem of the Nomex honeycomb core. The reason may be the ratio between the elastic modulus of the aramid paper and the phenolic resin is not low enough (the polymer substrates are 10^4 to 10^5-fold softer than the coating [53]).

3.5.3. Crushing stress

The crushing stress of the honeycomb may be calculated according to Eq. (7) below [54]:

$$\sigma^*_p = 3.21\sigma_y\left(\frac{\rho^*}{\rho_s}\right)^{\frac{5}{3}} \tag{8}$$

where the σ_y is the yield stress of the material of the honeycomb core.

Substituting both the tensile strength and compressive strength (2.13 MPa and 1.72 MPa, respectively) and the relative density (0.055) into Eq. (8), the crushing stress can be obtained as 0.054 MPa and 0.044 MPa, respectively. Both of them are much lower than the crushing stress of 1 MPa in this study. Perhaps, this crushing stress equation is not applicable to the honeycomb core with a very low relative density.

4. Numerical simulations

4.1. Mesh generation and boundary conditions

The numerical model of the honeycomb sandwich structure under flatwise compressive loading was developed using the commercial finite element code, ABAQUS/EXPLICIT [55], which is shown in Fig. 10. The facesheets are represented as two analytical rigid surfaces with an area of 60 mm × 60 mm. The honeycomb core with a cross-sectional area of 50.8 mm × 51.2 mm was explicitly modelled using shell elements (S4R) with hourglass-control and reduced integration.

After mesh sensitivity study, the mesh size is determined to be 0.185 mm × 0.185 mm, which means there are 10 elements on each edge of the honeycomb core. Thus, there are totally 977,400 elements and 956,148 nodes. Following the discussion before, the thickness of the single cell walls is taken as 0.07 mm and that of the double cell walls is 0.128 mm in the numerical modelling.

The motions of the two rigid surfaces were governed by the motions of the two reference points, RP-1 and RP-2, respectively. The Ref-2 was fixed in all 6 DOFs (*Ux, Uy, Uz, Rx, Ry* and *Rz*) and the RP-1 was fixed in two translational directions (*Ux* and *Uy*) and all three rotational directions (*Rx, Ry* and *Rz*). Here, the load

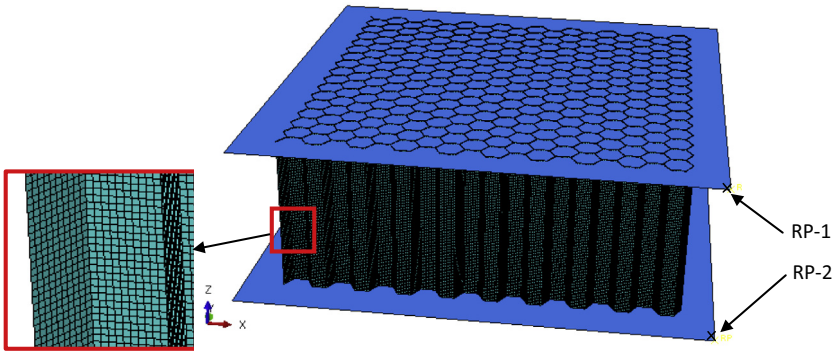

Fig. 10. Finite element model of the honeycomb sandwich. (a) 20 mm high honeycomb core, (b) 14 mm high honeycomb core.

was applied through a downward displacement of 18 mm in the RP-1 in *Uz* direction.

4.2. Contact relationships

The "Tie" constraints were used to simulate the fully-bonded conditions between honeycomb core and the two facesheets. The penalty and "hard" contact methods were used to define the tangential and normal interaction behaviour of the possibly self-contact among the walls of the core during compression, and the friction coefficient between the honeycomb cell walls was set to be 0.4 [50,56,57].

4.3. Constitutive model and failure criterion

The cell walls of the honeycomb core were modelled as laminas. Here, the single cell wall is a multi-layer structure of two resin layers and an aramid paper layer, with each resin layer of 0.008 mm thick and paper layer of 0.054 mm thick. The aramid paper layer is understandably placed between the two resin layers. The modelling of the double cell wall is similar, with the only difference of the aramid paper layer being 0.108 mm thick.

Aramid paper was modelled as an elasto-perfectly plastic material [39,45], and its compressive strength is assumed to be the same as its tensile counterpart. Phenolic resin is a brittle material, whose strengths in tension and compression were taken as 60 MPa and 180 MPa, respectively [50,58,59]. The phenolic resin was modelled as an elastic-brittle material and, in this model, the strength of the resin decreases from 180 MPa to a quite small value of 10 MPa after the compressive stress exceeds 180 MPa.

If the loading rate (displacement rate) in the explicit modelling is set to the same as that in testing (0.2 mm/min), it will be time intensive. Through trial studies, it was found that the loading (or displacement) rate of 1 mm/s or less would have a limited dynamic effect on the calculation results.

4.4. Simulation results and discussion

The comparison of the load–displacement relationships between the simulation and the test results is shown in Fig. 11. In general, the finite element output gives a reasonably good agreement with the experimental crushing response, especially to the 20 mm high core. The discrepancy during the hardening for the 14 mm high core (Fig. 11(b)) may be caused by underestimating of interaction between the cell walls, which likely shows a more severe contact in a core with a lower height for a given displacement.

The out-of-plane deformations of the cell walls in Y direction (the Y direction is shown in Fig. 10) at different compression stages

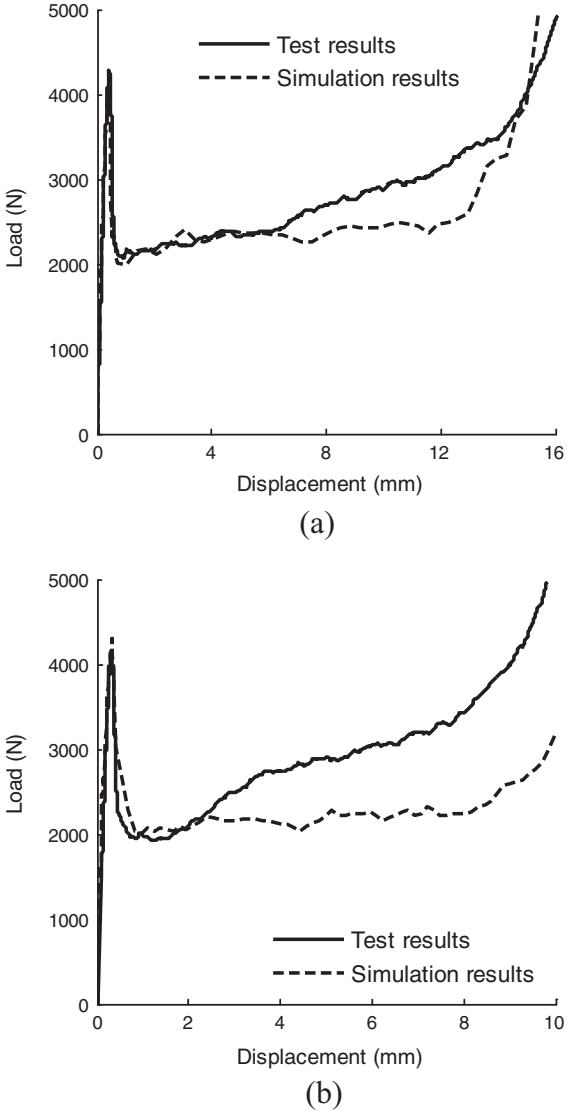

Fig. 11. Comparison of the simulated and tested load–displacement curves of honeycomb core sandwich subject to flatwise compression. (a) Front view: displacement = 0.3 mm, (b) front view: displacement = 0.41 mm, (c) front view: displacement = 1 mm, (d) front view: displacement = 0.41 mm.

are shown in Fig. 12, which are corresponding to the compressive displacements from 0 mm to 1 mm along Z direction (Fig. 10). As shown in Fig. 12(a), the cell walls start to buckle when the

compressive displacement is about 0.3 mm and reach the ultimate failure at the displacement of 1 mm. However, the maximum out-of-plane deformation of the cell walls is about 0.08 mm, and it is difficult to be observed just by naked eyes during the tests. Fig. 12(b) shows the collapse failure occurs and distributes randomly among the cell walls as the compressive displacement is about 0.41 mm. Fig. 12(c) shows that the failure increases with the increase of the compression. Fig. 12(d) shows that the maximum out-of-plane deformation in Y direction of the cell walls around the perimeter and in the middle of the honeycomb core are 0.8 mm and 0.1 mm respectively, which indicates the cell walls around the circumference fail firstly.

5. Parametric studies

5.1. Resin volume

The resin volume in the honeycomb core is influenced by the resin dipping times in the manufacturing process, the density and geometry of the core with aramid paper.

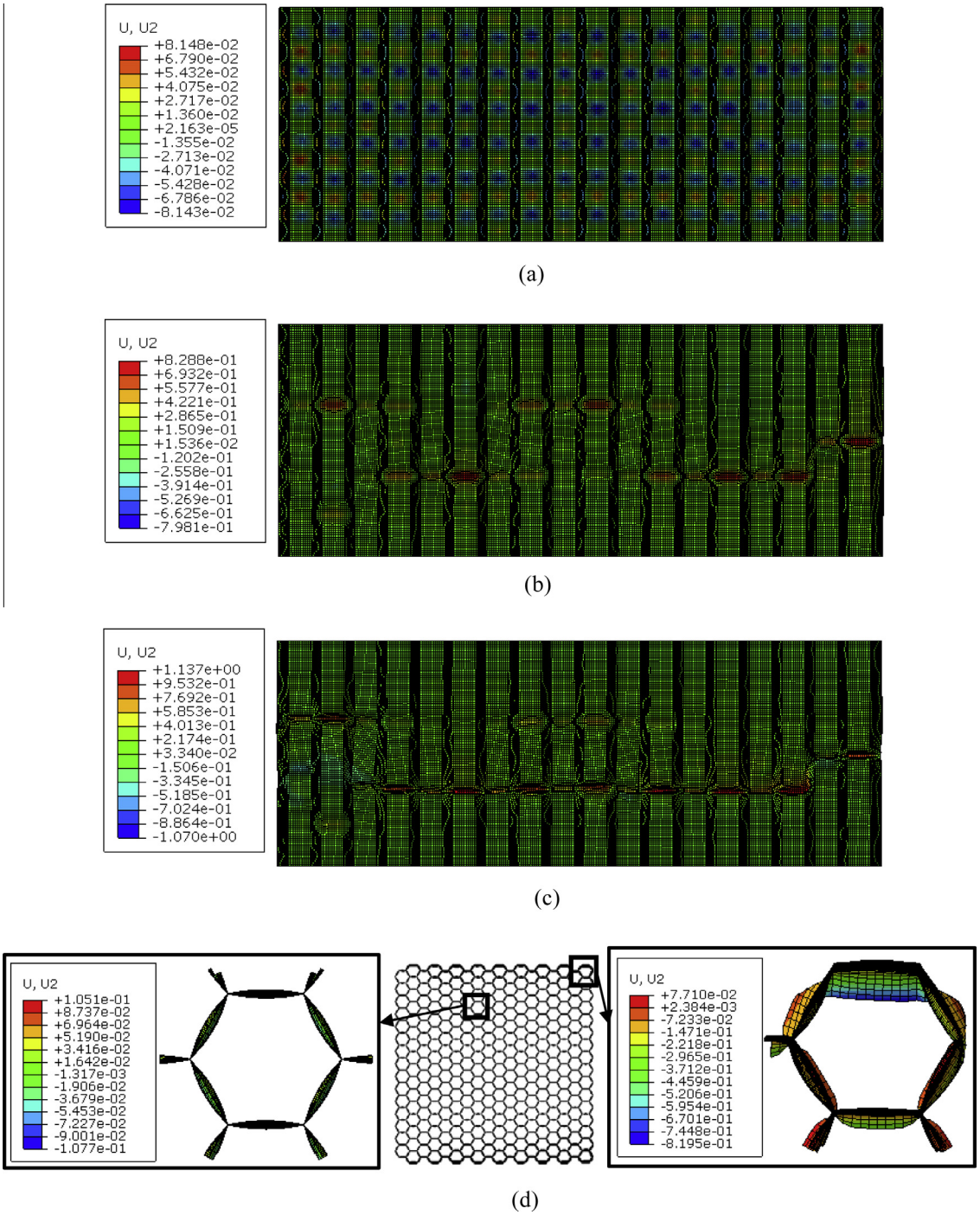

Fig. 12. Numerical results of the honeycomb core under transverse loading (all displacements in mm).

Table 2
The collapse load of the honeycomb core with different resin volume.

Resin thickness (mm)	0.004	0.006	0.008	0.01	0.012
Density (kg/m^3)	41.14	44.49	47.84	51.19	54.54
Collapse load (N)	3113	3771	4482	5460	6160
Displacement (mm)	0.41	0.41	0.41	0.41	0.41

Table 3
The collapse load of the honeycomb core with different resin's elastic modulus.

Modulus of resin (MPa)	4000	4500	5000	5500	6000
Collapse load (N)	4276	4397	4482	4592	4694
Collapse displacement (mm)	0.50	0.46	0.41	0.37	0.36

Table 4
The collapse load of the honeycomb core with different compressive strengths of resin.

Compressive strength of resin (MPa)	160	170	180	190	200
Collapse load (N)	4213	4349	4482	4606	4795
Collapse displacement (mm)	0.37	0.39	0.41	0.44	0.47

As for the 20 mm high honeycomb core, the collapse loads and the related displacements related to different resin layer thickness were simulated using the validated numerical model. The simulation results are illustrated in Table 2. It can be seen that the collapse loads increase greatly with the increase of the resin volume and however, the collapse displacements are all about 0.41 mm.

5.2. Resin property

The phenolic resin used to coat the aramid paper can also be varied. Again, as an example for the 20 mm high honeycomb core, the collapse loads and the related displacements with resin of different elastic modulus were simulated, which are shown in Table 3. From the table, it can be seen that the collapse loads increase with the increase of elastic modulus of the resin. However, the collapse displacements decrease with such the increase, as expected, due to increasing stiffness.

In addition, the collapse loads and the related displacements of the cores with resin of different compressive strengths were modelled, which are exhibited in Table. 4. It can be seen that both the collapse loads and collapse displacements increase with the increase of the compressive strength.

6. Conclusions

Tensile, stabilized compressive and step-by-step compressive tests have been conducted to study the material properties and mechanical response of the Nomex honeycomb core under transverse loading. A meso-scale finite element model with the representation of the cell wall structures has been developed to investigate the influence of the resin on the collapse behaviour of the honeycomb core. Through the analysis, the following conclusions may be drawn:

(1) The primary failure cause of the honeycomb core under transverse loading is the brittle fracture of the resin coating. The unloaded honeycomb core can almost recover to its original configurations if the unloading occurs before the densification phase. This is because the failure stain of the aramid paper is quite high and the aramid paper does not break after the core crush. The brittle failure of the resin often occurs randomly around the middle of the cell walls.

(2) The equivalent tensile stiffness of the honeycomb core is higher than the equivalent compressive stiffness, since the cell walls in this study are very thin and will buckle at a low loading level. The equivalent tensile strength of the core is higher than the equivalent collapse stress. Also, the local buckling of the honeycomb cell walls leads to local brittle fractures of the resin coating, which leads to the collapses of the honeycomb core.

(3) The increase of stabilized crushing load in the crushing phase is due to not only the air pressure increase inside the honeycomb core, but also the structural responses of the honeycomb sandwich under compression, such as the possible contact support and the friction between the cell walls.

(4) The honeycomb cores with different heights (14 mm and 20 mm in this study) have the same collapse strength and collapse strain.

(5) The majority of the existing theoretical estimations of the collapse strength and crushing strength are not adequate for predicting the mechanical behaviour of the honeycomb cores with excellent elastic aramid paper substrate and brittle phenolic-resin coatings.

(6) The volume of the resin coating has a positive effect on the collapse strength of the honeycomb core, but has no influence on the collapse strain. Also, the modulus of the resin coating has a positive effect on the collapse strength of the core, but has a negative effect on the collapse strain. In addition, the strength of the resin coating has positive effects on both the collapse strength and collapse strain of the honeycomb core.

Acknowledgements

The authors would like to acknowledge the DuPont Company for providing necessary technical data, and the authors would also like to appreciate the use of the cluster computers at School of Engineering in University of Liverpool for carrying out the calculation work in this study. The project was supported by Shanghai Municipal Natural Science Foundation (14ZR1422500).

References

[1] US Department of Transportation and Federal Aviation Adminstration. AMT Airframe Handbook, vol. 2 (FAA-H-8083-31). <https://www.faa.gov/regulations_policies/handbooks_manuals/aircraft/amt_airframe_handbook/>.

[2] Heimbs S, Schmeer S, Middendorf P, Maier M. Strain rate effects in phenolic composites and phenolic-impregnated honeycomb structures. Compos Sci Technol 2007;67:2827–37.

[3] Asprone D, Auricchio F, Menna C, Morganti S, Prota A, Reali A. Statistical finite element analysis of the buckling behaviour of honeycomb structures. Compos Struct 2013;105:240–55.

[4] Ratcliffe JG, Czabaj MW, Jackson WC. A Model for simulating the response of aluminum honeycomb structure to transverse loading. In: Proceedings of the American society for composites-27th technical conference, Arlington, Texas; 1–3 October 2012.

[5] Heimbs S. Virtual testing of sandwich core structures using dynamic finite element simulations. Comput Mater Sci 2009;45:205–16.

[6] Giglio M, Manes A, Gilioli A. Investigations on sandwich core properties through an experimental–numerical approach. Compos Part B-Eng 2012;43:361–74.

[7] Roy R, Nguyen KH, Park YB, Kweon JH, Choi JH. Testing and modeling of Nomex™ honeycomb sandwich panels with bolt insert. Compos Part B-Eng 2014;56:762–9.

[8] Heimbs S, Middendorf P, Hampf C, Hahnel F, Wolf K. Aircraft sandwich structures with folded core under impact load. In: Eighth international conference on sandwich structures (ICCS8), Feup, Porto; 2008. p. 369–80.

[9] Cvitkovich MK, Jackson WC. Compressive failure mechanisms in composite sandwich structures. J Am Helicopter Soc 1999;44(4):260–8.

[10] Kim CG, Jun E. Impact resistance of composite laminated sandwich plates. J Compos Mater 1992;26:2247–61.

[11] Zhou G, Hill M, Loughlan J, Hookham N. Damage characteristics of composite honeycomb sandwich panels in bending under quasi-static loading. J Sandw Struct Mater 2006;8(1):55–90.
[12] Abrate S. Localized impact on sandwich structures with laminated facings. Appl Mech Rev 1997;50(2):69–82.
[13] Lacy TE, Hwang Y. Numerical modeling of impact-damaged sandwich composites subjected to compression-after-impact loading. Compos Struct 2003;61:115–28.
[14] Aktay L, Johnson AF, Kroplin BH. Numerical modelling of honeycomb core crush behaviour. Eng Fract Mech 2008;75:2616–30.
[15] Gibson LJ, Ashby MF. Cellular solids: structures and properties. Pergamon Press; 1999.
[16] Wilbert W, Jang WY, Kyriakides S, Floccari JF. Buckling and progressive crushing of laterally loaded honeycomb. Int J Solids Struct 2011;48:803–16.
[17] Xu S, Beynon JH, Ruan D, Lu G. Experimental study of the out-of-plane dynamic compression of hexagonal honeycombs. Compos Struct 2012;94:2326–36.
[18] Miller W, Smith CW, Evans KE. Honeycomb cores with enhanced buckling strength. Compos Struct 2011;93:1072–7.
[19] Liang S, Chen HL. Investigation on the square cell honeycomb structures under axial loading. Compos Struct 2006;72:446–54.
[20] Mujika F, Pujana J, Olave M. On the determination of out-of-plane elastic properties of honeycomb sandwich panels. Polym Test 2011;30:222–8.
[21] HexWeb® honeycomb attributes and properties. Hexcel Corporation. Stamford, CT; 1999.
[22] Karakoc A, Santaoja K, Freund J. Simulation experiments on the effective in-plane compliance of the honeycomb materials. Compos Struct 2013;96:312–20.
[23] Foo CC, Chai GB, Seah LK. Mechanical properties of Nomex material and Nomex honeycomb structure. Compos Struct 2007;80:588–94.
[24] Castanié B, Aminanda Y, Bouvet C, Barrau JJ. Core crush criterion to determine the strength of sandwich composite structures subjected to compression after impact. Compos Struct 2008;86:243–50.
[25] Aminanda Y, Castanie B, Barrau JJ, Thevenet P. Experimental and numerical study of compression after impact of sandwich structures with metallic skins. Compos Sci Technol 2009;69:50–9.
[26] Aminanda Y, Castanie B, Barrau JJ, Thevenet P. Experimental analysis and modelling of the crushing of honeycomb cores. Appl Compos Mater 2005;12:213–27.
[27] Castanié B, Bouvet C, Aminanda Y, Barrau JJ, Thevenetd P. Modelling of low-energy_low-velocity impact on Nomex honeycomb sandwich structures with metallic skins. Int J Impact Eng 2008;35:620–34.
[28] Burton WS, Noor AK. Assessment of continuum models for sandwich panel honeycomb cores. Comput Methods Appl Mech Eng 1997;145:341–60.
[29] Aktay L, Johnson AF, Holzapfel M. Prediction of impact damage on sandwich composite panels. Comput Mater Sci 2005;32:252–60.
[30] McQuigg TD. Compression after impact experiments and analysis on honeycomb core sandwich panels with thin facesheets. NASA/CR-2011-217157; 2011.
[31] Zinno A, Prota A, Maio ED, Bakis CE. Experimental characterization of phenolic-impregnated honeycomb sandwich structures for transportation vehicles. Compos Struct 2011;93:2910–24.
[32] Aktay L, Johnson AF, Kroplin BH. Numerical modelling of honeycomb crush behaviour. Eng Fract Mech 2008;75(9):2616–30.
[33] Meo M, Morris AJ, Vignjevic R, Marengo G. Numerical simulation of low velocity impact on an aircraft sandwich panel. Compos Struct 2003;62:353–60.
[34] Besant T, Davies GAO, Hitchings D. Finite element modelling of low velocity impact of composite sandwich panels. Compos Part A-Appl Sci 2001;32:1189–96.
[35] Jiang D, Shu D. Local displacement of core in two-layer sandwich structures subjected to low-velocity impact. Compos Struct 2005;71:53–60.
[36] Chai GB, Zhu S. A review of low-velocity impact on sandwich structures. Proc Inst Mech Eng L-J Mater 2011;225:207–30.
[37] Sánchez-Sáez S, Barbero E, Navarro C. Analysis of the dynamic flexural behaviour of composite beams at low temperature. Compos Sci Technol 2007;67:2616–32.
[38] Foo CC, Chai GB, Seah LK. A model to predict low-velocity impact response and damage in sandwich composites. Compos Sci Technol 2008;68:1348–56.
[39] Hähnel F, Wolf K. Evaluation of the material properties of resin-impregnate NOMEX® paper as basis for the simulation of the impact behaviour of honeycomb sandwich. In: Third international conference on composite testing and model identification, Porto, Portugal; 2006.
[40] Horrigan DPW, Aitken RR, Moltschaniwskyj G. Modelling of crushing due to impact in honeycomb sandwiches. J Sandwich Struct Mater 2000;2:131–51.
[41] Buitrago BL, Santiuste C, Sánchez-Sáez S, Barbero E, Navarro C. Modelling of composite sandwich structures with honeycomb core subjected to high-velocity impact. Compos Struct 2010;92:2090–6.
[42] Giglio M, Gilioli A, Manes A. Numerical investigation of a three point bending test on sandwich panels with aluminum skins and Nomex™ honeycomb core. Comp Mater Sci 2012;56:69–78.
[43] Ivanez I, Sanchez-Saez S. Numerical modelling of the low-velocity impact response of composite sandwich beams with honeycomb core. Compos Struct 2013;106:716–23.
[44] Seemann R, Krause D. Numerical modelling of Nomex honeycomb cores for detailed analysis of sandwich panel joints. In: 11th World congress on computational mechanics (WCCM XI), fifth european conference on computational mechanics (ECCM V), sixth European conference on computational fluid dynamics (ECFD VI), Barcelona, Spain; 20–25 July 2014.
[45] Roy R, Park SJ, Kweon JH, Choi JH. Characterization of Nomex honeycomb core constituent material mechanical properties. Compos Struct. http://dx.doi.org/10.1016/j.compstruct.2014.06.033.
[46] Kim DS, Lee JR. Compressive mechanical properties of the Nomex/thermoset honeycomb cores. Polym Adv Technol 1997;8:1–7.
[47] Luo YQ, Wei H. Study on Properties of T722 Nomex honeycomb. Hi-Tech Fiber Appl 2009;34(1):34–7.
[48] ASTM international. ASTM C 365/C365M-11a: standard test method for flatwise compressive properties of sandwich cores. West Conshohocken, Pennsylvania, United States; 2011.
[49] ASTM international. ASTM C 297/C297M-04: standard test method for flatwise tensile strength of sandwich constructions. West Conshohocken, Pennsylvania, United States; 2011.
[50] NPCS board of consultants & engineers. Phenolic resins technology handbook, New Delhi: NIIR Project Consultancy Services; 2007.
[51] Zhang J, Ashby MF. The out-of-plane properties of honeycombs. Int J Mech Sci 1992;34(6):475–89.
[52] Wang Y. Elastic collapse of honeycombs under out-of-plane pressure. Int J Mech Sci 1991;33(8):637–44.
[53] Volynskii L, Bazhenov S, Lebedeva OV, Bakeev NF. Mechanical buckling instability of thin coatings deposited on soft polymer substrates. J Mater Sci 2000;35:547–54.
[54] Fan X, Verpoest I, Vandepitte D. Finite element analysis on out-of-plane compression properties of thermoplastic honeycomb. In: Proceedings of the seventh international conference on sandwich structures, Aalborg University, Aalborg, Denmark; 29–31 August 2005. p. 875–84.
[55] Hibbitt D, Karlsson B, Sorensen P. ABAQUS documents (version 6.12). Dassault Systemes Simulia Corporation, Providence, RI, USA; 2012.
[56] Kim SJ, Jang H. Friction and wear of friction materials containing two different phenolic resins reinforced with aramid pulp. Tribol Int 2000;33:477–84.
[57] Ren G, Zhang Z, Zhu X, Ge B, Guo F, Men X, et al. Influence of functional graphene as filler on the tribological behaviors of Nomex fabric phenolic composite. Compos Part A-Appl Sci 2013;49:157–64.
[58] Ratna D. Handbook of thermoset resins. Shropshire: Smithers Rapra Technology; 2009.
[59] Kilchert SV. Nonlinear finite element modelling of degradation and failure in folded core composite sandwich structures. Docterate Dissertation. University of Stuttgart; 2013.